Available online at www.sciencedirect.com
ScienceDirect
Engineering Applications of Artificial Intelligence 19 (2006) 753–760
Engineering Applications of
ARTIFICIAL
INTELLIGENCE
www.elsevier.com/locate/engappai

A signal-processing tool for non-destructive testing of inaccessible pipes

Francesca Cau, Alessandra Fanni*, Augusto Montisci, Pietro Testoni, Mariangela Usai

Department of Electrical and Electronic Engineering, University of Cagliari, Italy

Received 18 May 2006; accepted 21 May 2006
Available online 20 July 2006

Abstract

The design of Non-Destructive-Testing systems for fault detection in long and not accessible pipelines is an actual task in the industrial and civil environment. At this purpose, the diagnosis based on the propagation of guided ultrasonic waves along the pipes offers an attractive solution for the fault identification and classification. The authors studied this problem by means of suitable Artificial Neural Network models. Numerical techniques have been used to simulate the guided wave propagation in the pipes. In particular, the finite element method has been used to model different kinds of pipes and faults, and to obtain several returning echoes containing the faults information. Torsional wave modes have been used as excitation waves. The obtained signals have been processed in order to reduce the data dimensionality, and to extract suitable features. The features selected from the signals can be further processed in order to limit the size of the Neural Network models without loss of information. At this purpose, the principal component analysis has been investigated. Finally, the selected features have been used as input for the neural network models. In this paper, traditional feed-forward, multi-layer perceptron networks have been used to obtain the information on size and location of localized notches.

Keywords: Non-destructive testing; Finite element analysis; Neural networks; Fast Fourier transform; PCA

1. Introduction

The presence of flaws and corrosion in pipes is one of the major problems in industrial and civil plants, as water, oil, steam, and gas pipelines. The non-destructive testing (NDT) with ultrasonic-guided waves in the pipe wall provides an interesting solution to the fault-inspection problem. In fact, by positioning a ring transducer in only one point, usually accessible for inspections, it is possible to inspect long pipes without dismantling and interrupting the service, favouring the least uneasiness and economic loss (Lowe et al., 1988; Alleyne et al., 2001). At this purpose, particular ultrasonic-guided waves, called Lamb Waves (Cawley and Alleyne, 1996), can be excited at the edge of the pipe and will propagate many meters, returning echoes indicating the presence of faults, such as corrosion, cracks, notches, etc.

In this work, several tests have been performed by exciting the fundamental torsional mode in the pipe. The characteristics of this propagation mode are not affected by the presence of fluid in the pipes and there is no other axisymmetric torsional mode in the frequency range.

The diagnostic system proposed in this paper is based on artificial neural networks (NNs), for their ability of generalization and for the characteristic of not requiring any fault physical model. In particular, fault diagnosis has been modeled as a pattern recognition process in which the classifier is a NN. Classically, a pattern recognition system is indeed composed of three modules (Duda and Hart, 1973): a transducer that acquires data on the physical device; a feature extractor, whose purpose is to reduce the data dimensionality that the transducer produces, to filter the noise, and to compute significant features or properties; a classifier that makes a decision on the class whose the fault belongs to.

In the diagnostic system we propose in this paper, the transducer is made up of mechanically independent dry-coupled elements, which impose prescribed circumferential displacements on a number of nodes distributed around an accessible pipe section; the feature extractor are fast Fourier transform (FFT), principal component analysis

*Corresponding author. Tel.: +39 07067 55870; fax: +39 07067 55900.
E-mail address: fanni@diee.unica.it (A. Fanni).

0952-1976/$ - see front matter © 2006 Elsevier Ltd. All rights reserved.
doi:10.1016/j.engappai.2006.05.005

(PCA), and other preprocessing techniques usually adopted to suite the data to the chosen classifier; the classifier is a multi-layer perceptron (MLP) NN. This choice is corroborated by most of the literature, as reviewed in Fanni et al. (1999).

Basically, the main feature of a MLP resides in its intrinsic ability to perform extremely complex tasks in a very short time, once the learning phase has been completed. The networks have as many nodes in the input layer as the number of significant features extracted from the signals, while the number of output nodes depends on the fault coding chosen by the designer. In this paper, a linear coding is used to code the different geometrical parameters characterizing the faults.

Two main phases can be recognized in the diagnostic task: the training phase and the defect-detection phase.

During the defect-detection operations, the signals acquired on the actual pipe have to be preprocessed and used as inputs to the NN that has been previously trained using the numerical model of the pipe. Theoretically, it may be possible to use actual measurements in the training phase, but this is not practical. In fact, the data to feed the NNs during the training phase are the waves reflected by the defects. These signals can be obtained by a large amount of experimental tests, which consist in artificially building several faults of different dimension and location in a certain number of pipes. This process is very expensive, complex and time consuming, especially if various and numerous datasets are required. Thus, the alternative way consists of obtaining the required signals by using numerical analysis, e.g., the finite element method (FEM) (Reinhold and Lord, 1998). Also in this case, few data will be available and will have a large dimensionality. In fact, the solution of the numerical models requires a large amount of memory space and CPU time, as the pipelines to be studied can be several meters long and many features can characterize each signal. However, real acquisitions can be used in particular cases, e.g., to estimate the magnitude of the measurement noise. The use of a finite element code can substitute the experimental tests, providing signals, which are as close as possible to the real data.

As previously cited, in this paper, torsional wave mode excitations have been examined. The shape of a torsional mode is not frequency-dependent and it is completely non-dispersive. In fact, as specified in Demma et al. (2003), no other torsional mode is present in the used frequency range for both finite element models and experiments.

A sensitivity analysis has been performed to set up the model that guarantees to obtain signals with the highest informative content. Suitable wave modes and frequency have been chosen to produce the best penetration power according to bibliography.

Afterwards, external notches of different dimension and location have been considered.

The present research has been performed in collaboration with other Italian Universities. In particular, the database has been provided by the research group of the University of Pisa (Bertoncini and Raugi, 2005) and it has been achieved by using the commercial simulation code CAPA (CAPA WisSoft et al.).

2. The method

The use of model-free approaches for NDT, such as NNs, is justified by the difficulty of finding a proper solution to this problem by using analytical methods. The most widely used neural classifier is the MLP. A MLP NN is constituted by an input layer, one or more hidden layers, and one output layer of neurons. The neurons of each layer are connected with all the neurons of the previous layer. The connection weights are the free parameters of a learning process. They are determined by presenting to the network a set of actual input–output values (the training set) and searching the minimum of a suitable error function, which depends on the connections weights. To evaluate the network performances the trained network is applied to a new set of examples (the test set).

It can be noted that, if the number of examples in the training set is limited, as in the present problem, the network size (i.e., the number of connection weights) has to be limited, in order to avoid the overfitting of the network. This can be done by limiting the number of hidden layers, or the number of neurons in the hidden layers, or by reducing the number of input neurons. Since the number of input neurons has to be chosen according to the number of independent variables, i.e., the number of features used to describe the wave reflected by the defect, the feature extraction and selection procedure is crucial to limit the network size.

In the present paper, an MLP with one hidden layer has been chosen. As in the most of applications presented in literature, the size of hidden layer has to be heuristically determined.

A suitable training procedure has to be adopted to avoid overfitting and overtraining. Overfitting occurs when a network has too many degrees of freedom and therefore fits the examples in a more complicated fashion than necessary. Overtraining on the other hand even appears in optimally chosen network architectures if the task is nonlinear. As long as the number of examples is small, an overtrained network might learn the examples best, although it shows poor generalization abilities. To avoid overfitting, model selection strategies should be applied in order to choose the most adequate network architecture. In particular, the growing method has been adopted here. It consists on training a network having few neurons and then evaluating their performance. If such performance is satisfactory, the procedure ends, otherwise a new network having more hidden neurons is trained, and so on, until the network reaches the desired performance.

To avoid overtraining, a set of examples, called validation set, is left out of the training set. During the training phase, the mean square error, evaluated on the validation set, gives us information regarding the

overtraining. As the error on the validation set begins to rise, the training process terminates (early stopping).

To increase the resolution power of the model, limiting, at the same time, the number of input neurons, feature extraction and data reduction strategies have been adopted, as described in the following.

3. Numerical analysis

The theory of the elastic wave propagation in a hollow cylinder is based on the Navier's equations of motion in a cylindrical coordinate system (Barshinger et al., 2002):

$$\mu\nabla^2\mathbf{u} + (\lambda+\mu)\nabla(\nabla\cdot\mathbf{u}) = \rho\frac{\partial^2\mathbf{u}}{\partial t^2}, \tag{1}$$

with

$$\lambda = \frac{vE}{(1+v)(1-2v)} \tag{2}$$

and

$$\mu = \frac{E}{2(1+v)}, \tag{3}$$

where $\mathbf{u}$ is the displacement field, E is the Young's modulus of the material, v is its Poisson's modulus, ρ is its density and λ and μ are its Lamè's constants, determined by (2) and (3).

The differential equation (1) can be solved in boundary problems through a numerical approach. Finite element 3-D models have to be built in order to simulate the wave propagation in the pipes.

The key problem associated with the measurement of the propagating Lamb waves characteristics is that more than one mode can exist at any given frequency. In a NDT inspection system, selection and exploitation of a single mode is very important. In fact, generally, an excitation source can excite all the modes, which exist within its frequency bandwidth, resulting in a signal, which is much too complicated to interpret. Even with a single mode, great care is needed for correct identification of the echoes reflected by the defects and by normal pipe features such as welds. Therefore, it is essential to design the transducers and to choose the forcing signal in order to excite only the chosen mode. In fact, theoretical and experimental results show that suitable mode and frequency can be chosen to produce a better penetration power and to increase the quality of the results. In this paper, the fundamental torsional mode is excited in a pipe by prescribing the circumferential displacements of suitable nodes belonging to an accessible section. The excitation is a displacement signal applied in the extremity node of the model. It is a six-cycle tone burst enclosed in a Hanning window as described by (4) and reported in Fig. 1 (Jackson, 1995):

$$y = \sin(2\pi ft)\sin^2\left(\frac{2\pi ft}{12}\right). \tag{4}$$

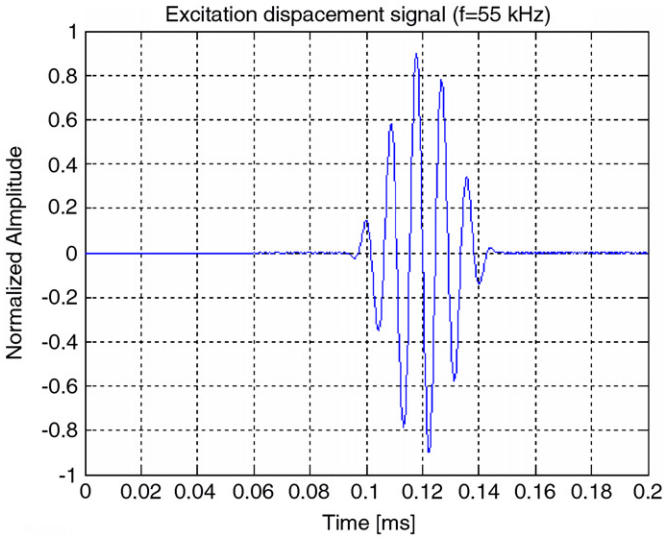

Fig. 1. Excitation displacement signal.

The parameter f is the excitation frequency chosen by the previous considerations.

The Hanning windowing is largely used to reduce the leakage, which occurs when the signals are not periodic in the temporal and spatial sampling window. The aliasing has been avoided by suitably sampling the data, according to bibliography (Lowe et al., 1988). This mode is very attractive for testing for several reasons:

- it is practically non-dispersive over a wide bandwidth around this frequency (its velocity does not vary significantly with frequency), so that the signal shape and amplitude are retained as it travels;
- it is the fastest mode so that any unwanted mode converted signal arrives after it has been received;
- its mode shape makes it equally sensitive to internal or external defects at any circumferential location.

The numerical analyses have been carried out simulating the MsSR—2020 *D* instrument, developed by SwRI South West Research Institute in San Antonio, Texas, and purchased by University of Pisa (Bertoncini and Raugi, 2005). The instrument is based on magnetostrictive sensor technology, and it can be arranged to generate and detect torsional waves in the pipe under test. In the examined cases, the transducer has been simulated as made up of 36 mechanically independent dry-coupled elements uniformly distributed around the exterior circumference, located in a section at a distance of 0.6 m from the edge of the pipe. The generated wave propagates in the pipe walls until it is reflected by a defect or a discontinuity. The returning echo is received by the same excitation transducer, which also works as a survey probe.

In the following, a detailed description of the three-dimensional model used to generate our synthetic data is reported. Data have been generated by simulating propagation and scattering of torsional elastic waves in a pipe

Table 1
Geometrical dimensions and material properties of the modelled pipe

Length of the pipe	2.1 m
Outer radius	0.043 m
Thickness	0.0055 m
Young's modulus	215.7 GN/m^2
Poisson's coefficient	0.300
Density	7850 kg/m^3

Table 2
Model element dimensions and sampling time

Number of axial subdivisions	1420
Number of radial subdivisions	5
Number of circumferential subdivisions	36
Sampling time (ms)	3.03×10^{-4}
Excitation frequency (kHz)	55

with notches having different geometrical dimensions. The transient numerical analysis has been carried out by the FEM.

The geometrical dimensions and the characteristics of the pipe are shown in Table 1.

A sensitivity analysis of the pipe model without defects has been firstly performed. The purpose of this test is to set the simulation parameters, i.e., the dimensions of the elements in the FEM model, and the sampling time. By decreasing the sampling time (or the element length), the precision of the results increases, but the simulation process time increases too. A compromise has to be found between these contrasting requirements (Cau et al., 2005).

The sampling time identifies the instants in which the solution is calculated; moreover, a sub-sampling has to be done, namely only one sample data every two has been stored; this operation allows us to reduce the storage memory, preserving the informative content of the signals.

The dimensions of the elements in the FEM model, and the sampling time are shown in Table 2.

3.1. Dataset

The second part of the numerical study concerns the simulation of a pipe with different notches in the external wall. Varying the location and the dimensions of the defect, several simulations have been performed.

The geometry of the test pipe is reported in Fig. 2. The notch axial position, axial length, thickness, and angular amplitude have been varied as reported in Table 3, resulting in a data set composed by 300 defect cases. The limited number of simulations is due to the high CPU time required for each of them.

In the dataset, the signal that refers to the pipe without defect is included in order to improve the classification results. Thus, the dataset is composed by $D = 301$ simulations: 300 defect cases and the fault free case.

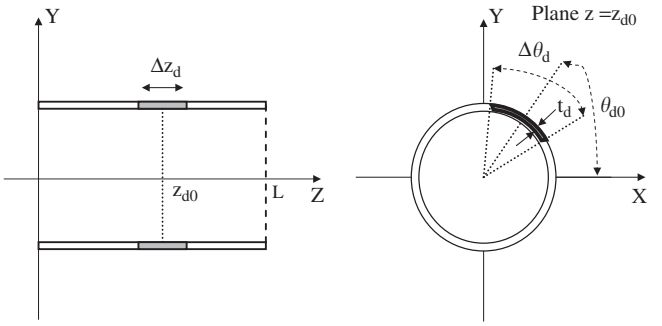

Fig. 2. Geometry of the inspected pipe: L is the length of the pipe; $z_{d0}$is the defect axial position; Δz_d is the defect axial length; θ_{d0} is the defect angular position; $\Delta\theta_d$ is the defect angular amplitude; t_d is the defect thickness.

Table 3
Geometric fault characteristics

	Range
Defect axial position z_{d0} (m)	1, 1.4, 1.8, 2.2
Defect angular position θ_{d0}(deg)	0°
Defect thickness t_d (mm)	0.55, 1.65, 2.75, 3.85, 4.95
Defect axial length Δz_d (mm)	3, 6, 12, 18, 24
Defect angular amplitude $\Delta\theta_d$ (deg)	20°, 40°, 60°

For each defect, the used signals are the torsional components of the displacement wave, measured in the 36 observing points, and defined as in (Bertoncini and Raugi, 2005):

$$u_t(t,\theta_n,\theta_{d0}) = -u_x(t,\theta_n,\theta_{d0})\sin(\theta_n) + u_y(t,\theta_n,\theta_{d0})\cos(\theta_n), \quad (5)$$

where

- $u_x(t;\theta_n;\theta_{d0})$ and $u_y(t;\theta_n;\theta_{d0})$ are the Cartesian components of the displacement in the X–Y plane in Fig. 2;
- $\theta_n = (n-1)10°, n = 1,2,\ldots,N$ is the angular position of the generic observing point;
- $N = 36$ is the number of the observing points;
- θ_{d0} is the angular position of the defect.

In order to reduce the data dimensionality, the reflected waves obtained from the numerical simulations have been surveyed only during prefixed time windows. In particular, a time window of 0.14 s has been chosen, twice the excitation signal time period. This time window contains 460 samples. In Fig. 3 the reflected signals corresponding to defects with $z_{d0} = 1$ m, $t_d = 4.95$ mm, $\Delta\theta_d = 40°$, and $\Delta z_d = 3$ mm, $\Delta z_d = 12$ mm, and $\Delta z_d = 24$ mm, respectively, are reported, in the corresponding time windows.

In general, if D is the number of different performed simulations ($D = 301$ in the present paper), S is the number of samples in the chosen temporal window ($S = 460$ in the present paper), and N is the number of observing points

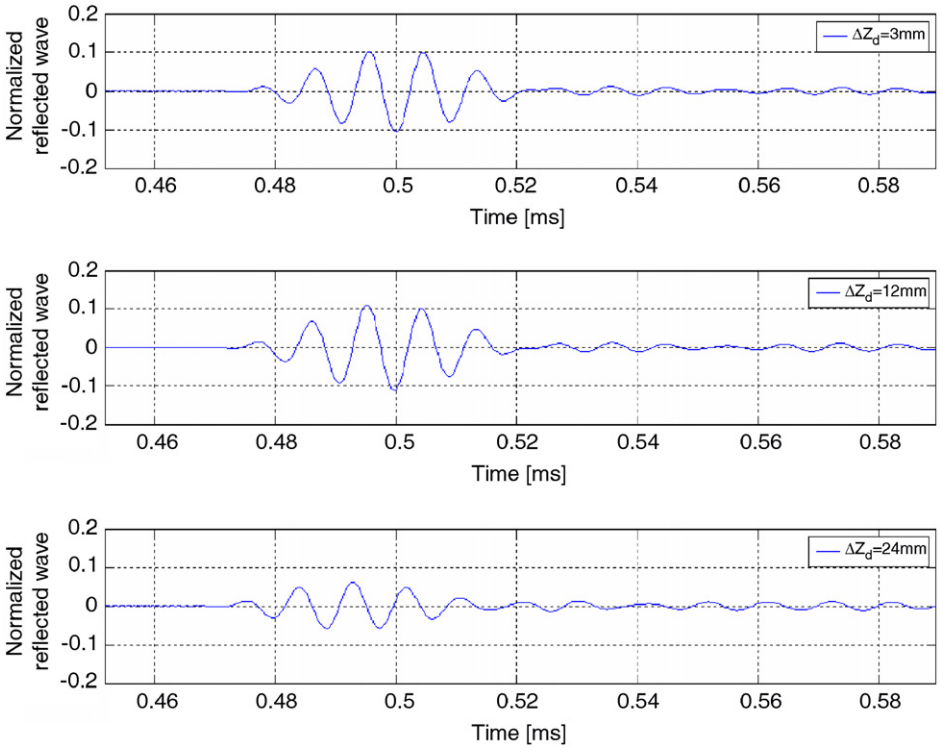

Fig. 3. Reflected waves corresponding to defects with $z_{d0} = 1$ m, $t_d = 4.95$ mm, $\Delta\theta_d = 40^\circ$, and $\Delta z_d = 3$ mm, $\Delta z_d = 12$ mm, and $\Delta z_d = 24$ mm, in the chosen time window.

along the circumference of the pipe ($N = 36$ in the present paper), D different matrices of dimension ($S \times N$) can be built, each of them characterizing a particular defective pipe or the pipe without defect. Each matrix, which represents the pattern describing the corresponding defect, has been processed (as detailed in the following) in order to generate input patterns suitable to be fed to the NN classifier. The corresponding output pattern will be constructed associating to the input pattern the corresponding coding of the defect.

As outlined, some post processing is necessary on the D matrices, in order to extract significant features and to reduce the data dimensionality. Moreover, to improve separability between patterns, different normalization techniques have been applied, as described in the following. Normalization prevents the subsequent pattern recognition from being biased by signals with larger response magnitude.

3.2. Features extraction and data reduction

A two-dimensional FFT (FFT-2D) has been applied to each of the D matrices, obtaining D new couples of matrices, $\underline{\underline{A}}_d(s,n)$ and $\underline{\underline{P}}_d(s,n)$, containing the amplitude and the phase components of the FFT. In fact, it has been verified that the defect thickness influences the FFT amplitude, while the defect axial length influences the shape of the waves, and, consequently, the FFT phase (Demma et al., 2003; Oppenhein and Lim, 1981).

To reduce the data dimensionality, a subset of K amplitude components has been selected from $\underline{\underline{A}}_d$. In order to perform the choice of these components, the D amplitude matrices are summed up. The K-selected components are those whose value, in the sum matrix, is greater than the threshold defined in (6):

$$threshold = 0.02\left(\max\left(\sum_d \underline{\underline{A}}_d(s,n)\right)\right);$$
$$s = 1,\ldots,S; \quad n = 1,\ldots,N; \quad d = 1,\ldots,D. \tag{6}$$

The coefficient 0.02 in the threshold definition has been chosen with a trial and error procedure.

The selected K amplitude components of all the D matrices $\underline{\underline{A}}_d$ have been stored in a unique matrix of dimension ($K \times D$), and the corresponding phase components have been stored in a further matrix of the same dimension. In the present case, K is equal to 74. These two matrices have been normalized so that they have means of zero and standard deviations of 1.

PCA has been then applied to the FFT amplitude matrix and to the FFT phase matrix.

PCA method consists of orthogonalizing the components of the input data in such a way that they are uncorrelated one to each other, ordering the resulting orthogonal components (principal components) and finally eliminating those that contribute the least to the variation in the data set. The Signal-Processing Toolbox of MatlabR12 has been used. This routine employs singular

value decomposition to compute the principal components (Signal Processing Toolbox for MATLAB R12, 2004).

The PCA procedure eliminates the principal components that contribute less than a prefixed percentage to the total variation in the data set (1% in the present paper). The remaining principal components (9 for the amplitude matrix and 8 for the phase matrix, in the present case) have been selected. Finally, by projecting each column of the amplitude and phase matrices on the principal components, and merging the resulting reduced matrices, the input matrix has been obtained, which has $9+8$ rows and D columns. In the present paper, the input matrix has been reduced to (17×301), with a very limited loss of information. Note that each column of the matrix represents an input pattern to the NN, as 17 are the significant features representing the defect/fault free case, and 301 are the defective cases plus the fault-free case considered.

The corresponding output matrix has four rows containing the defect values: defect axial length ΔZ_d (mm); defect angular amplitude $\Delta\theta_d$ (deg); defect thickness t_d (mm); defect axial position Z_{d0} (m). The output matrix has as many columns as the number of defect/faulty free simulations, i.e., it has D columns.

In order to suit the data to the NNs, the input and the output matrices have been normalized in the interval $[-1, 1]$.

The resulting data set has been divided in three sets: the training set, the validation set, and the test set. The validation and the test sets have been obtained by extracting a number of defect cases from the dataset. In particular, in the present paper, one matrix column each six has been extracted from the input and the output matrices, i.e., 30 defect cases have been selected to construct the test set, 30 defect cases constitute the validation set, while the remaining 241 defect cases constitute the training set. Note that the extracted defect cases, both for validation and test, are representative of the entire defect domain.

A further problem to manage is the exiguity of the defect simulations, and consequently the exiguity of the input training patterns. In order to increase the training set, two further matrices have been generated from the original input training matrix. Each matrix element has been obtained by adding to each element of the original input training matrix a value randomly chosen in a range $[-0.001, 0.001]$. This range has been chosen by calculating the minimal variation among column in the input training matrix, and reducing this value to about a half. This procedure is so able to take into account the noise in the actual measurements. The new augmented input training matrix, whose dimension is (17×723), is obtained by joining these two matrices to the original matrix. The output-training matrix has been generated by repeating the original output-training matrix three times.

3.3. NN classifiers

The experimental results showed that the relationship between the defect axial position z_{d0} and the return time of the reflected wave is quite linear (Cau et al., 2005). For such reason, the determination of the defect axial position has not been included among the task of the neural classifier.

The following MLP architecture has been used to predict the defect axial length Δz_d, the defect angular amplitude $\Delta\theta_d$, and the defect thickness t_d:

- 17 input nodes;
- one hidden layer with 20 nodes and hyperbolic tangent activation function;
- three output nodes corresponding to the dimension of the defect axial length, of the defect angular amplitude, and of the defect thickness respectively. The output nodes activation functions are linear.

The network has been trained using the Levenberg–Marquard learning algorithm.

The stopping criteria consist of a maximum number of 500 epochs, a minimum error gradient and a minimum mean square error, evaluated in the training set, equal to 10E-5. The training phase stops if one of these criteria is met, or if early stopping occurs.

The number of input neurons is imposed by the previously described features selection procedure, while the number of hidden neurons, as in the most of applications presented in literature, has been heuristically determined. In particular, the growing method has been adopted, as described in Section 2.

3.4. Results

The following results refer to the classification errors evaluated on the test set.

Fig. 4 shows the percentage errors, while Fig. 5 compares the actual values of the defect angular amplitude with the values predicted by the neural classifier. As can be noted, the classifier performance is very good: the percentage classification mean error, evaluated over all the test set, is equal to 1.8%, while the test set is predicted with an error less than 10% in more than 96% of the cases.

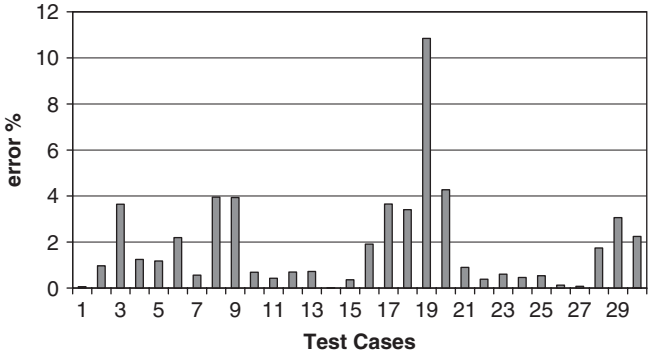

Fig. 4. Defect angular amplitude classification: percentage errors distribution of the test set.

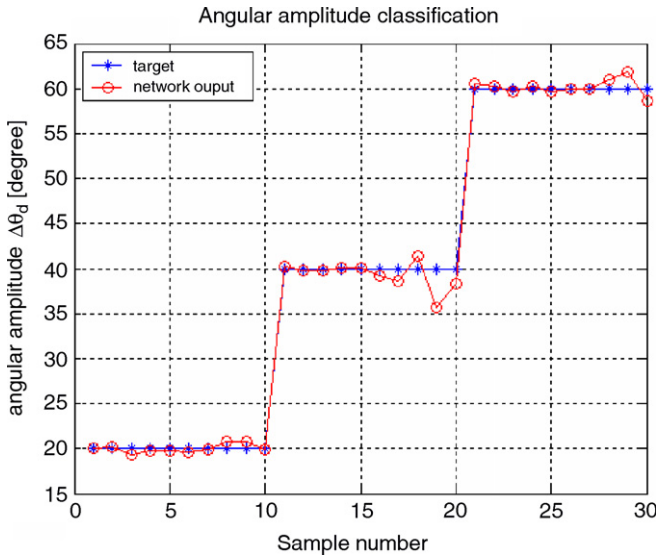

Fig. 5. Defect angular amplitude classification: comparison between actual values and values predicted by the neural classifier.

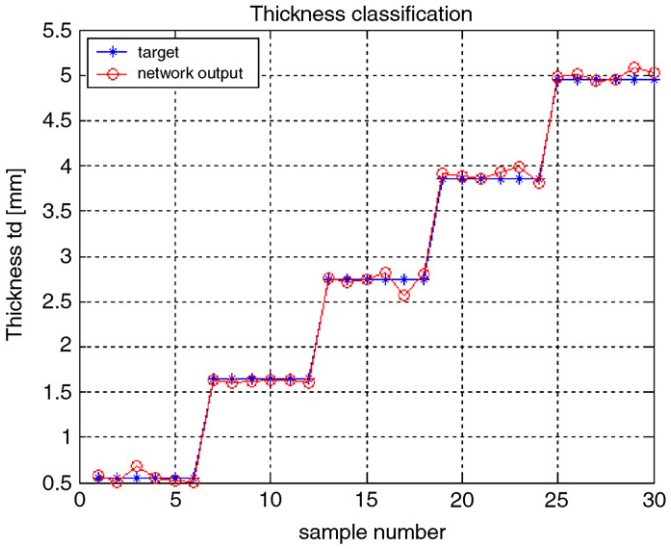

Fig. 7. Defect thickness classification: comparison between actual values and values predicted by the neural classifier.

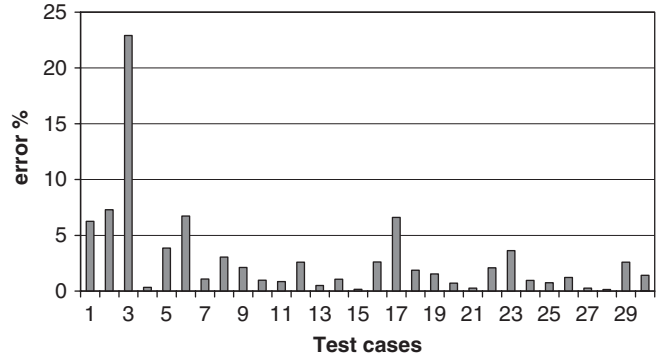

Fig. 6. Defect thickness classification: percentage errors distribution of the test set.

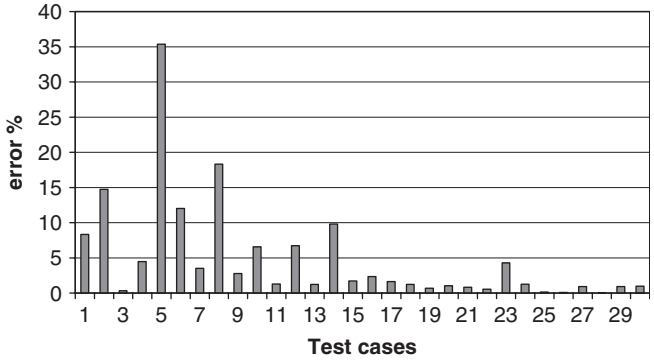

Fig. 8. Defect axial length classification: percentage errors distribution of the test set.

Fig. 6 shows the percentage errors, while Fig. 7 compares the actual values of the defect thickness with the values predicted by the neural classifier. Also in this case, the classifier performance is quite good: the percentage classification mean error, evaluated over all the test set, is equal to 2.9%, while only in one case the test set is predicted with an error greater than 10%.

Fig. 8 shows the percentage errors, while Fig. 9 compares the actual values of the defect axial length with the values predicted by the neural classifier. In this case, the classifier performance is acceptable: the percentage classification mean error, evaluated over all the test set, is equal to 4.8%, while the test set is predicted with an error less than 10% in more than 85% of the cases.

The computation time of each test case is of the order of 20 ms, as it requires only simulating the neural classifier. On the contrary, the computation time of each numerical simulation performed by the commercial tool CAPA (Bertoncini and Raugi, 2005) is of the order of 2 h. This limits the number of examples to be used in the training of

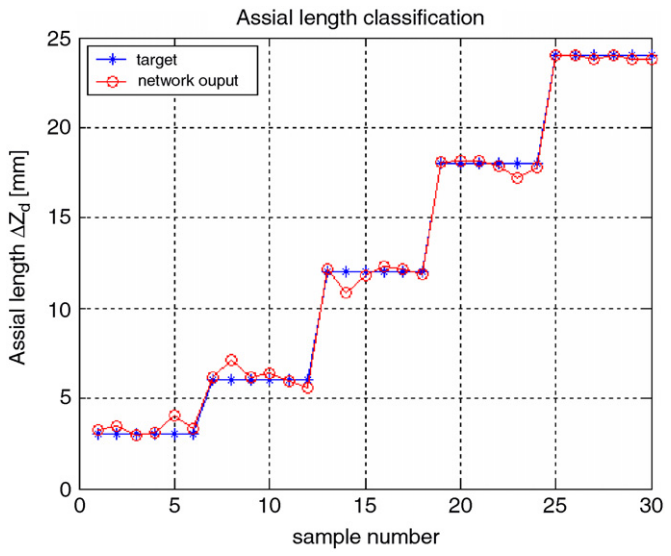

Fig. 9. Defect axial length classification: comparison between actual values and values predicted by the neural classifier.

the neural classifier. This limit has been overcome by the various feature extraction, data reduction, and data augmentation procedures proposed in the paper.

4. Conclusions

A diagnostic system based on neural networks for non-destructive testing with ultrasonic waves in not accessible pipes has been implemented. The signal dataset for the training, validation and test has been synthetically obtained by using the finite element method. The signals are preprocessed with FFT, and PCA techniques to obtain input data suitable to be used as input to neural networks.

Torsional wave mode has been excited on the pipe affected by realistic non-symmetric faults with different axial position, axial length, angular amplitude, and thickness.

Preliminary analyses of the numerically simulated defects show that the return time of the reflected signal linearly depends on the defect position, while it is independent on the entity of the fault. The notch position is therefore determined with precision only from the knowledge of this time value.

The obtained classification error distributions for defect angular amplitude, defect thickness, and defect axial length are very encouraging, showing the suitability of the proposed approach to the development of a signal processing package for NDT instrument.

The obtained results have to be validated with actual measures. This paper represents indeed a preliminary contribution to the realization of an intelligent and flexible tool for non-destructive testing of inaccessible pipes.

Acknowledgments

The work was supported by the Italian Ministry of Education under the PRIN Program.

The authors would like to thank M. Raugi and F. Bertoncini, both with the Department of Electric Systems and Automation, University of Pisa, Italy, for providing the FEM simulations used here, and for the useful discussions.

The authors also thank the anonymous Reviewers for the valuable comments in improving the quality of this paper.

References

Alleyne, D.N., Pavlakovi, B., Lowe, M.J.S., Cawley, P., 2001. Rapid long range inspection of chemical plant pipework using guided waves. Insight 43, 93–96.

Barshinger, J., Rose, J.L., Avioli Jr., M.J., 2002. Guided wave resonance tuning for pipe inspection. Journal of Pressure Vessel Technology 124, 303–310.

Bertoncini, F., Raugi, M., 2005. Numerical and experimental analysis of long range guided waves for nondestructive testing of pipes. Proceedings of the WEAS/IASME International Conference on Systems Theory and Scientific Computation, pp. 108–113.

CAPA WisSoft, Buckenhof, Germany-Release: 4.1.

Cau, F., Fanni, A., Montisci, A., Testoni, P., Usai, M., 2005. Artificial neural networks for non desctrutive evaluation with ultrasonic waves in not accessible pipes. Proceedings of the IEEE Conference on Industry Applications 1, 685–692.

Cawley, P., Alleyne, D.N., 1996. The use of lamb waves for the long-range inspection of large structures. Ultrasonics 34, 287–290.

Demma, A., Cawley, P., Lowe, M., 2003. The reflection of the fundamental torsional mode from cracks and notches in pipes. Journal of the Acoustical Society of America 114, 611–625.

Duda, R.O., Hart, P.E., 1973. Pattern Classification and Scene Analysis. Wiley, New York.

Fanni, A., Giua, A., Marchesi, M., Montisci, M., 1999. A Neural Network Diagnosis Approach for Analog Circuits, Applied Intelligence, vol. 11. Kluwer Academic Pub., Dordrecht, pp. 169–186.

Jackson, L.B., 1995. Digital Filters and Signal Processing. Kluwer Academic Publishers, Dordrecht.

Lowe, M.J.S., Alleyne, D.N., Cawley, P., 1988. Defect detection in pipe using guided waves. Ultrasonics 36, 147–154.

Oppenhein, A., Lim, J.S., 1981. The importance of the phase in Signals. Proceedings of the IEEE 69, 529–541.

Reinhold, L., Lord, W., 1998. A finite-element formulation for the study of Ultrasonic NDT Systems. IEEE Transactions on Ultrasonics, Ferroelectrics and Frequency Control. 35, 809–820.

Signal Processing Toolbox for MATLAB R12, 2004.